Search for B_s^0 oscillations using inclusive lepton events

The ALEPH Collaboration

Abstract

A new search for B_s^0 oscillations is performed in a sample of semileptonic B hadron decays collected by the ALEPH experiment during 1991–1995. Compared to previous inclusive lepton analyses, the proper time resolution and mistag rate are significantly improved. In addition subsamples of the data are assigned an enriched or depleted B_s^0 fraction. Maximum likelihood fits are performed to derive a preliminary lower limit of $\Delta m_s > 10.2$ ps^{-1} at 95% CL. Combining with the ALEPH D_s^- based analyses yields $\Delta m_s > 10.4$ ps^{-1} at 95% CL.

Submitted to the 1997 lepton-photon conference, Hamburg

1 Introduction

The small mass difference between the mass eigenstates of the B_s^0 meson causes oscillations between the B_s^0 and $\bar{B}_s^0$ flavour states with frequency Δm_s. Within the framework of the Standard Model a measurement of the ratio $\Delta m_s/\Delta m_d$ (Δm_d being the B_d^0 oscillation frequency) would allow the extraction of $|V_{ts}/V_{td}|$ where V_{ts} and V_{td} are elements of the Cabibbo-Kobayashi-Maskawa (CKM) quark mixing matrix.

Although the slow B_d^0 oscillations are now well established, the faster B_s^0 oscillations still remain to be measured. Previous ALEPH analyses searching for B_s^0 oscillations have either been based on semi-exclusive selections in which a D_s^- is fully reconstructed [1, 2] or on more inclusive lepton selections [3, 4, 5]. Although the latter suffer from a lower B_s^0 purity and poorer proper time resolution they have the advantage of larger statistics.

The new analysis presented here is also based on an inclusive lepton sample, but, compared to the previous ALEPH inclusive lepton analysis [4], a number of improvements are made to increase the sensitivity to B_s^0 mixing:

- **Initial and final state tagging:** The "optimal tagging method" [1], previously used only for the D_s^- based analyses, is applied; a tagging efficiency of 100% and an improved mistag rate are obtained. In addition, with this method, the mistags and the sample composition are estimated on an event-by-event basis.

- **B_s^0 enrichment:** Various properties of the events, such as the charge of the reconstructed B vertex, are used to enrich the fraction of B_s^0 in subsamples of the data.

- **Decay length resolution:** An improved decay length resolution is obtained by applying tight selection cuts to remove events likely to have misassigned tracks between the primary and the B_s^0 vertex.

  In addition the decay length error is used on an event-by-event basis, rather than assuming a constant decay length error for all events as was done previously.

- **Boost resolution:** An improved algorithm is used for the estimation of the momentum of the B hadrons.

The rest of this paper proceeds to give further details of these improvements and is organised as follows. In Section 2 the event selection is described. The next section explains the B_s^0 enrichment procedure. The following two sections explain the proper time reconstruction and the procedure for tagging the initial and final state. Section 6 and 7 present the likelihood function and the results. In Section 8 the systematic uncertainties are estimated, and some additional checks of the analysis performed. Finally in the last section the combination of this analysis with the ALEPH D_s^- based analyses is described.

2 Event selection

This analysis uses approximately 4 million hadronic events recorded by the ALEPH detector from 1991 to 1995 at centre of mass energies close to the Z mass, and selected with the charged particle requirements described in Ref. [8]. It also relies on Monte Carlo samples of fully simulated $Z \to q\bar{q}$ events. The Monte Carlo generator is based on JETSET 7.4 [6] with updated branching ratios; the Körner-Schuler model [7] is used for semileptonic B hadron decays.

The event is required to have the thrust axis away from the beam axis ($|\cos\theta_{thrust}| < 0.85$). The event is then split into two hemispheres using the plane perpendicular to the thrust axis. Using the standard ALEPH lepton selection criteria [9], events containing one or more identified electron or muon with momentum above 3 GeV/c are kept. The leptons are then associated to their closest jet (JADE algorithm with $y_{cut} = 0.004$) and a transverse momentum p_T with respect to the jet is calculated with the lepton momentum removed from the jet. Only hemispheres containing a lepton with $p_T > 1.25$ GeV/c are selected. In the case that more than one lepton in an event satisfies this requirement, only the lepton with the highest momentum is used as a B^0_s candidate.

Next the charm vertex in the event is reconstructed. Charged particles which are in the lepton hemisphere (excluding the lepton) are assigned to either the interaction point or a single reconstructed displaced vertex. A three-dimensional grid point search is performed for the secondary vertex position to find the displaced vertex point-track assignment combination that has the greatest difference in χ^2 when compared to the case where all tracks are assumed to come from the interaction point. Tracks are required to come within 3σ of their assigned vertex. All tracks assigned to the charm vertex, with momentum above 1.5 GeV/c and within 1.4σ of the vertex are then combined to form a reconstructed charm track. If only one track passes this condition it serves as the charm track. If no tracks are found or none of the tracks in the charm vertex have a vertex detector hit the event is rejected. The charm track is then intersected with the lepton to form a candidate B^0_s vertex. The lepton is required to have a vertex hit and the χ^2 per degree of freedom of the reconstructed B vertex is required to be less than 25.

The following additional cuts are applied:

- the momentum of the charm track greater than 4 GeV/c. This cut is increased to 8 GeV/c when the angle between the charm track and the lepton is less than 10°;
- the reconstructed mass of the B hadron (calculated as described in Section 4) less than 8 GeV/c^2;
- the missing energy in the B^0_s hemisphere greater than -2 GeV;
- the angle between the charm track and the lepton between 5° and 30°;
- the angle between the charm track and the jet less than 20°.

Although these additional cuts reduce the event sample by 60%, the average decay length resolution of the remaining events is improved by a factor 2 and the amount of non-B background in the sample reduced by a factor 3. In addition the average momentum resolution of the sample is improved. A total of 33000 events survive after all cuts.

Table 1: Values of the physics parameters and their uncertainty assumed in this analysis.

Physics parameter	Value and uncertainty	Reference
B^+ lifetime	1.65 ± 0.04 ps	[10]
B^0_d lifetime	1.55 ± 0.04 ps	[10]
B^0_s lifetime	1.52 ± 0.07 ps	[10]
b-baryon lifetime	1.21 ± 0.06 ps	[10]
Δm_d	0.466 ± 0.019 ps^{-1}	[11]
$f_{B^0_s} = \mathcal{B}(\bar{b} \to B^0_s)$	$0.105^{+0.016}_{-0.015}$	[11]
$f_{B^0_d} = f_{B^+} = \mathcal{B}(\bar{b} \to B^0_d, B^+)$	$0.394^{+0.016}_{-0.020}$	[11]
$f_{b-baryon}$	$0.106^{+0.037}_{-0.027}$	[11]
$\mathcal{B}(b \to \ell)$	0.1116 ± 0.0020	[12]
$\mathcal{B}(b \to c \to \ell)$	0.0797 ± 0.0034	[12]
$\mathcal{B}(b \to \bar{c} \to \ell)$	0.108 ± 0.0042	[12]
$\mathcal{B}(c \to \ell)$	0.098 ± 0.005	[13]
ϵ_b	$0.0037^{+0.0014}_{-0.0008}$	[13]

Table 2: Composition of the inclusive lepton sample(%). The error is the statistical uncertainty from the Monte Carlo.

B^0_s	B^0_d	other B-hadrons	charm	uds
10.56 ± 0.09	38.38 ± 0.13	47.65 ± 0.14	2.22 ± 0.07	1.19 ± 0.05

3 B^0_s enrichment

Assuming the physics parameters listed in Table 1 and the reconstruction efficiencies determined from the Monte Carlo, the composition of the event sample is estimated to be that shown in Table 2 with an overall B^0_s fraction of 10.6%.

Monte Carlo studies show that the sensitivity of the analysis to B^0_s mixing, can be increased by splitting the data into subsamples containing an enriched or depleted B^0_s fraction. A total of eleven classes are therefore constructed based on the track multiplicity at the charm vertex, the number of identified kaon candidates and the charge correlation between the tracks at the charm vertex and the lepton. The definition of the classes is given in Table 3. As the last class contains those events which do not satisfy the criteria of the preceeding classes, the enrichment procedure is 100% efficient.

For the classes requiring the presence of kaon candidates, the following criteria are used: momentum above 2 GeV/c and $\chi_\pi + \chi_K < 0$ and $|\chi_K| < 2$, where χ_π (χ_K) are the dE/dx estimators, defined as the difference between the measured and expected ionisation in the time projection chamber expressed in terms of standard deviations for the π (K) mass hypothesis.

Table 3: Definition of the eleven B_s^0 purity enrichment classes. Column 1 indicates the number of charged tracks at the charm vertex. Column 2 indicates whether the charge of these tracks are the same (S) or opposite (O) to that of the decay lepton, the tracks being ranked in order of decreasing momentum. Column 3 indicates the subclasses based on the presence of kaon candidates or consistency with the ϕ mass. Column 4 indicates the relative fraction of the data events in each class. Column 5 indicates the B_s^0 purity in each class as estimated from Monte Carlo. Column 6 indicates the effective weight of that class in the analysis.

No. tracks	Charge	Kaon requirements	Fraction (%)	B_s^0 purity (%)	Weight
1	O	1 kaon	3.8 ± 0.1	24.5 ± 0.6	0.21
		0 kaon	14.9 ± 0.2	15.0 ± 0.3	0.30
2	OS, SO	$1.01 < m_\phi < 1.03$ GeV/c^2	1.2 ± 0.1	21.5 ± 1.0	0.05
	OS, SO	0 kaon	17.8 ± 0.2	7.1 ± 0.2	0.08
	OS, SO	1 kaon	17.4 ± 0.2	5.3 ± 0.2	0.04
	OS, SO	2 kaons	2.3 ± 0.1	8.5 ± 0.5	0.01
	OO		8.3 ± 0.2	17.0 ± 0.4	0.21
3	OOS		2.9 ± 0.1	19.7 ± 0.7	0.10
	OSO		3.8 ± 0.1	18.5 ± 0.5	0.11
	SOO		3.9 ± 0.1	14.9 ± 0.5	0.08
rest			23.6 ± 0.2	5.8 ± 0.1	0.07

For the case of a one- or three-track charm vertex the enrichment procedure works because a neutral B vertex is more likely to be a B_s^0. For events having two tracks at the charm vertex, the B_s^0 purity of 8.6% is lower than the overall average, as these events are more likely to originate from a charged B vertex. For this large subsample of events (47%), the presence of kaon candidates, consistency with the ϕ mass and requirement that the charge of the highest momentum track and the lepton be opposite provide additional enrichment. Monte Carlo studies indicate that this enrichment procedure is effectively equivalent to increasing the statistics of the sample by $28\% \pm 3\%$.

4 Proper time reconstruction

The reconstructed proper time of each event $t = g\ell$ is estimated from the measured decay length (ℓ) and boost term (g). The boost term is calculated as $g = m_B/p_B$ where $m_B = 5.3$ GeV/c^2 is the assumed B mass and p_B the reconstructed momentum.

The decay length is calculated as the distance from the primary vertex to the B vertex projected onto the direction of the jet associated to the lepton. Figure 1a shows the decay length resolution for all B events, the RMS decay length resolution is 480 μm. An event-by-event decay length uncertainty σ_l is also estimated for each event from the covariance matrices of the tracks attached to the vertices.

The B momentum is estimated as $p_B = \sqrt{(E_c + E_\nu + E_\ell)^2 - m_B^2}$ where E_c is the

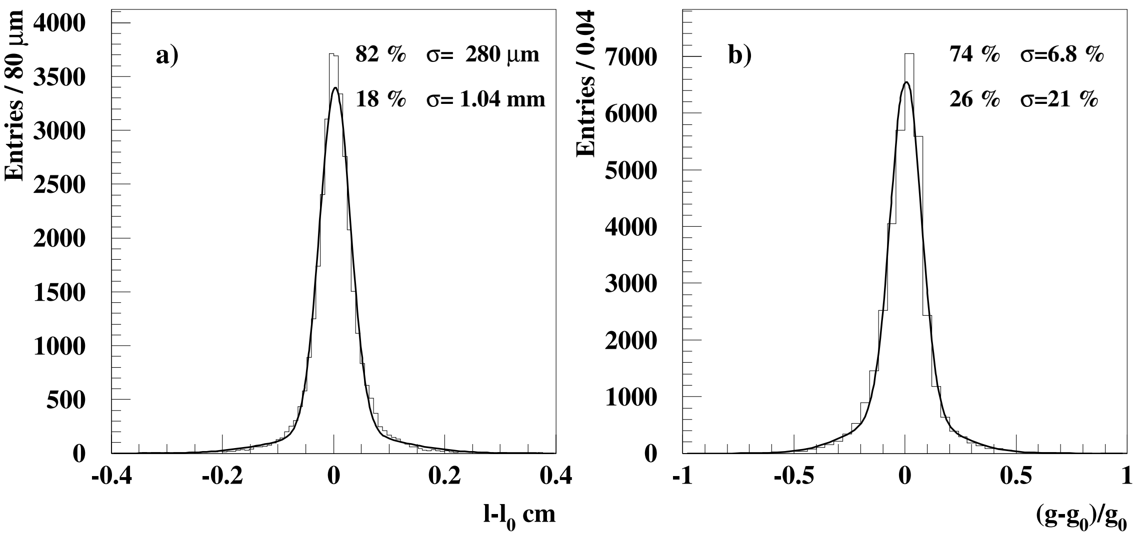

Figure 1: For all B hadrons: (a) the decay length resolution (ℓ_o is the true decay length), (b) the relative boost term resolution (g_0 is the true boost term). The curves are the result of fits to the sum of two Gaussians whose relative fractions and widths are indicated.

energy of the charm particle, E_ν the neutrino energy and E_ℓ the lepton energy. The charm particle energy is calculated by clustering a jet (using the JADE algorithm) around the charged tracks at the charm vertex until a mass of 2.7 GeV$/c^2$ is reached. To reduce the influence of fragmentation particles in the E_c estimate, charged and neutral particles with energy less than 0.5 GeV are excluded from the clustering. The neutrino energy is estimated as the missing energy in the lepton hemisphere taking into account the measured mass in both hemispheres [14]. Figure 1b shows the boost term resolution for B events obtained with this method.

Assuming the direction of flight of the B hadron is the same as that of its associated jet, an estimate of the B mass can be calculated from the energy of the neutrino and the four-vectors of the charm particle and the lepton. This is the mass used in the selection cuts.

In the likelihood an event-by-event proper time error

$$\sigma_t^{\alpha\beta} = \sqrt{(gS_\ell^{dat}S_\ell^\alpha\sigma_\ell)^2 + (tS_g^\beta)^2} \tag{1}$$

is used. Here S_ℓ^α ($\alpha = 1, 2$) are correction factors which are applied to take into account that the pull distribution for the decay length resolution is not exactly Gaussian with unit width: a fit of the sum of two Gaussians to the distribution of $(\ell - \ell_0)/\sigma_l$ in the Monte Carlo yields a fraction $f_\ell^1 = 0.85$ with a sigma $S_\ell^1 = 1.3$ and a fraction $f_\ell^2 = 0.15$ with $S_\ell^2 = 4.3$. The factors S_g^β ($\beta = 1, 2$) for the boost term resolution are obtained by fitting $(g - g_0)/g_0$ to the sum of two Gaussians; the results are indicated in Fig. 1b.

The constant $S_\ell^{dat} = 1.06 \pm 0.10$ takes into account that the decay length uncertainty measured in data is slightly larger than that obtained from the Monte Carlo. It has been determined using a fake leptons sample, as described in [3].

Figure 2 shows the proper time resolution obtained for various intervals of true proper time.

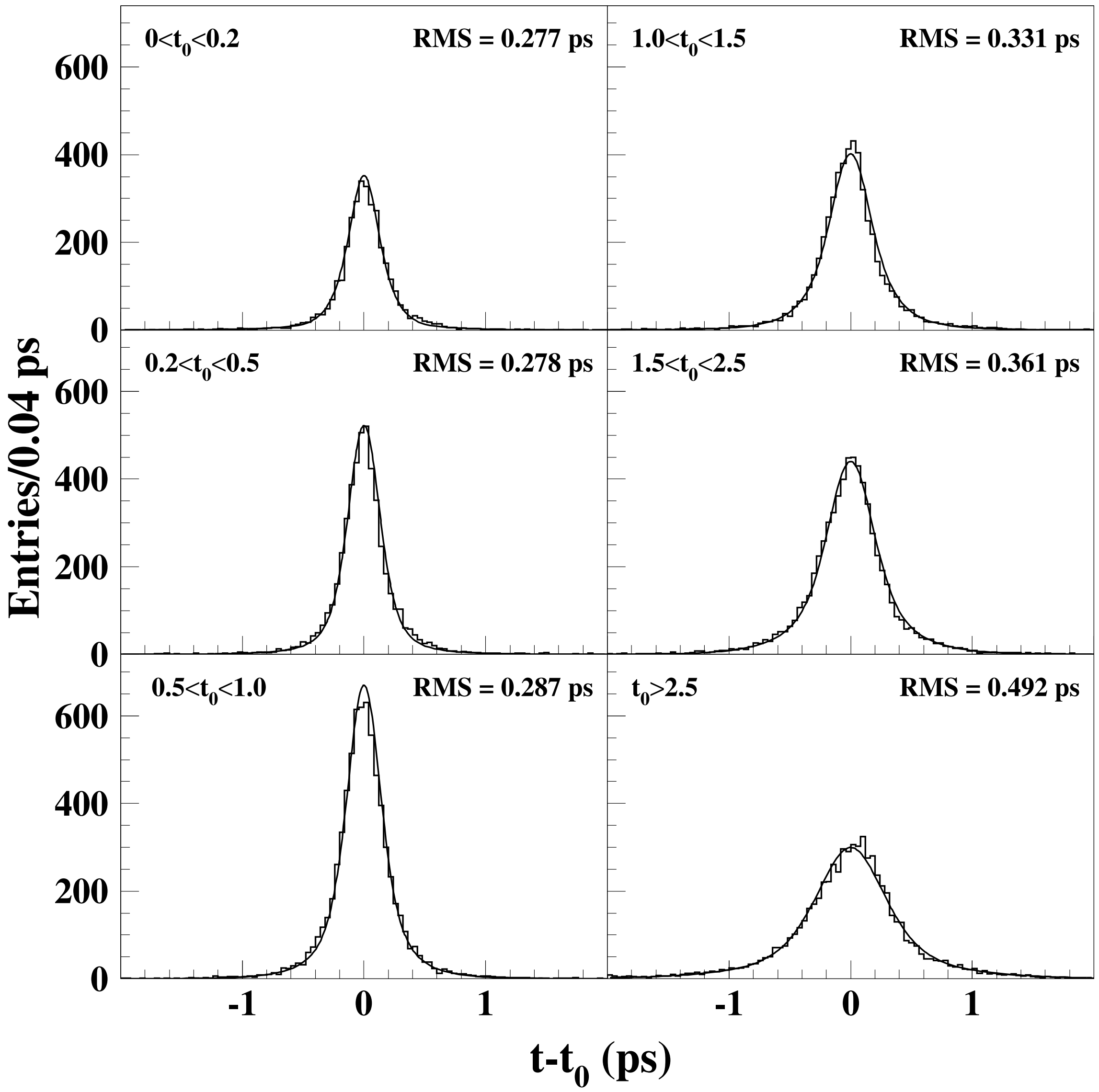

Figure 2: The proper time resolution for B events in various intervals of true proper time t_0 (in ps). The curves display the corresponding resolution assumed in the likelihood as obtained from Eq. (1).

5 Initial and final state tagging

The flavour state of the decaying B_s^0 is estimated from the charge of the reconstructed lepton. This final state tag is incorrect if the lepton is from $b \to c \to \ell$ (5.9% of the B events in the sample) as in this case the charge of the lepton is reversed. The flavour state at production time is estimated using a variety of initial state tags. The power of these tags is enhanced by the means of discriminating variables which have some ability to distinguish whether or not the tag is correct. This approach was first used in the ALEPH D_s^--lepton analysis [1] and further details can be found there.

A B_s^0 candidate is "tagged as unmixed (mixed)" when the reconstructed initial and final flavour states are the same (different). By definition, candidates from $c\bar{c}$, uds, or non-oscillating B backgrounds are only "correctly tagged" if they are "tagged as unmixed".

For each B_s^0 candidate, one of the tags described below is used to determine the initial state.

- **Lepton tag:** Leptons with momentum greater than 3 GeV/c are searched for in the hemisphere opposite to the B_s^0 candidate. The sign of the lepton with the highest transverse momentum $p_t(l_o)$ tags the nature of the initial b quark in the opposite hemisphere. It takes precedence over the other tags if it is available.

- **Fragmentation kaon tag:** The fragmentation kaon candidate is defined as the highest momentum charged track within 45° of the B_s^0 direction identified, using the vertexing algorithm described in Section 2, as being more likely to come from the primary vertex than the B_s^0 vertex, and satisfying $\chi_K < 0.5$ and $\chi_K - \chi_\pi > 0.5$.

  The sign of the fragmentation kaon candidate tags the sign of the b quark in the same hemisphere. It is used if no opposite hemisphere lepton tag is found.

- **Opposite hemisphere charge tag:** The opposite hemisphere charge is defined as

$$Q_{\mathrm{o}} = \frac{\sum_i^{oppo} q_i \, |p_{||}^i|^\kappa}{\sum_i^{oppo} |p_{||}^i|^\kappa}, \tag{2}$$

  where the sum is over all charged particles in the opposite hemisphere, $p_{||}^i$ is the momentum of the i^{th} track projected on the thrust axis, q_i its charge and $\kappa = 0.5$. The sign of Q_{o} tags the initial state of the b quark in the opposite hemisphere. This tag is always available but has the largest mistag probability of the three tags. It is used only if no other tag is available.

The events are sorted into five exclusive classes based on the availability and results of the three tags. The definition of these tagging classes and the list of the discriminating variables associated with each class are given in Table 4. The variable Q_{s} is the sum of the charges of all the tracks in the same hemisphere and carries information on the initial state of the B_s^0. As the sum of charges of tracks originating from the decay of a neutral particle is zero, it is independent of whether the B_s^0 decays as a B_s^0 or a $\bar{B}_s^0$. The variable Z_K is the fraction of the available beam energy taken by the fragmentation kaon

Table 4: The tag and discriminating variables used in each class. The quantities $S(Q_o)$, $S(K)$ $S(\ell_o)$ and $S(\ell_s)$ are the signs of the opposite hemisphere charge, the fragmentation kaon and the opposite and same side leptons. Classes 3-5 all use the sign of the opposite hemisphere lepton as the initial state tag. For class 3 no fragmentation kaon candidate is identified. For class 4 (class 5) a fragmentation kaon candidate is found whose charge is opposite to (the same as) the charge of the opposite hemisphere lepton.

Tagging class	1	2	3	4	5
Initial state tag	Q_o	K	l_o	l_o	l_o
$\|Q_o\|$	YES	no	no	no	no
$S(Q_o)Q_s$	YES	no	no	no	no
$S(K)Q_o$	no	YES	no	no	no
$S(K)Q_o$	no	YES	no	no	no
χ_π	no	YES	no	YES	YES
Z_K	no	YES	no	YES	YES
$S(l_o)Q_o$	no	no	YES	YES	YES
$S(l_o)Q_s$	no	no	YES	YES	YES
$p_T(l_o)$	no	no	YES	YES	YES
t	no	YES	no	YES	YES
$p_T(l_s)$	YES	YES	YES	YES	YES
Fraction (DATA) %	71.4 ± 0.2	11.9 ± 0.2	14.2 ± 0.2	1.3 ± 0.1	1.2 ± 0.1
B_s^0 purity %	10.0 ± 0.1	13.3 ± 0.3	10.3 ± 0.2	15.8 ± 1.0	12.1 ± 0.8
B_s^0 mistag %	38.6 ± 0.5	28.8 ± 1.0	34.0 ± 1.1	16.1 ± 2.3	56.1 ± 3.5
B_s^0 effective mistag %	31.9	24.6	24.1	13.7	26.2

candidate (as defined in Ref. [1]). The inclusion of the reconstructed B_s^0 proper time t takes into account that the mistag probability of the fragmentation kaon increases as the B_s^0 vertex approaches the primary vertex, due to the misassignment of tracks between the primary and secondary vertices. The inclusion of the $p_t(\ell_s)$ of the lepton from the B_s^0 in all tagging classes reduces the effect of $\mathcal{B}(b \to c \to \ell)$ on the final state mistag.

The signal mistag probability η, as well as the probability distributions for correctly and incorrectly tagged signal events ($r_i(x_i)$ and $w_i(x_i)$) of each discriminating variable x_i, are estimated from the $Z \to q\bar{q}$ Monte Carlo.

The various discriminating variables chosen in each class, $x_1, x_2, \ldots$, are combined into a single effective discriminating variable $x^{\rm eff}$, according to the prescription developed for the D_s^- based analyses [1, 2]. This new variable is defined as

$$x^{\rm eff} = \frac{\eta\, w_1(x_1)\, w_2(x_2)\, \cdots}{(1-\eta)\, r_1(x_1)\, r_2(x_2)\, \cdots + \eta\, w_1(x_1)\, w_2(x_2)\, \cdots}, \qquad (3)$$

and takes values between 0 and 1. A small value indicates that the B_s^0 oscillation is likely to have been correctly tagged.

The probability density functions $G_{jk}^c(x^{\rm eff})$ of $x^{\rm eff}$ are determined for each lepton source j and in each tagging class k, separately for the correctly ($c = +1$) and incorrectly ($c = -1$) tagged events. This determination (as well as the estimation of the corresponding mistag probabilities η_{jk}) is based on Monte Carlo events. The functions $G^c_{jk}(x^{\rm eff})$ are found to be similar for all B hadron sources and therefore assumed to be equal for these sources.

The enhancement of the tagging power provided by the variable $x^{\rm eff}$ depends on the difference between the $G^+_{jk}(x^{\rm eff})$ and $G^-_{jk}(x^{\rm eff})$ distributions, and can be quantified in terms of effective mistag rates, as described in Ref. [1]. The effective mistag rates for the B^0_s signal in the five tagging classes are given in Table 4. As the sign of the decay lepton is used when determining the oscillation state, these mistags include the effect of $b \to c \to \ell$ on the final state mistag. Finally the average B^0_s effective mistag is 28.9 %.

6 Likelihood function

Each B hadron source has a different probability distribution function for the true proper time t_0 and for the discrete variable λ, defined to take the value -1 for the mixed case or $+1$ for the unmixed case. Assuming CP conservation and equal lifetime for the two CP eigenstates in each neutral B meson system, the joint probability distribution of the true proper time t_0 and λ can be written as

$$p_j(\lambda, t_0) = \frac{e^{-t_0/\tau_j}}{2\tau_j} \left[1 + \lambda \cos\left(\Delta m_j \, t_0\right)\right] , \tag{4}$$

where τ_j and Δm_j are the lifetime and oscillation frequency of B hadron source j (with the convention that $\Delta m_j = 0$ for non oscillating B hadrons). The joint probability distribution of the reconstructed proper time t and of λ is obtained as the convolution of $p_j(\lambda, t_0)$ with the four Gaussians used to parametrize the lifetime resolution (see Sect. 4):

$$h_j(\lambda, t) = \sum_{\alpha=1}^{2} \sum_{\beta=1}^{2} f_\ell^\alpha f_g^\beta \left[\frac{1}{\sqrt{2\pi}\sigma_t^{\alpha\beta}} \int_0^\infty e^{-\left[\frac{t-t_0}{\sqrt{2}\sigma_t^{\alpha\beta}}\right]^2} p_j(\lambda, t_0)\, dt_0 \right] \tag{5}$$

For the $c\bar{c}$ and uds backgrounds, $h_{jl}(-1, t) = 0$ since these sources are unmixed by definition, and $h_{jl}(+1, t)$ are just the reconstructed proper time distributions. These distributions are determined from Monte Carlo samples and are parametrized as the sum of Gaussian functions.

The likelihood function used in this analysis is based on the values taken by four different variables in the selected data events. These variables are the reconstructed proper time t and its error σ_t, the tagging result μ, taking the value -1 for events tagged as mixed or $+1$ for those tagged as unmixed, and the effective discriminating variable $x^{\rm eff}$. The use of the discriminating variable $x^{\rm eff}$ in this likelihood function is reduced to the use of two sets of functions of $x^{\rm eff}$, $X_{jk}(x^{\rm eff})$ and $Y_{jkl}(x^{\rm eff})$, whose values can be interpreted as event-by-event mistag probabilities and fractions of the different lepton sources respectively. The likelihood of the total sample is written as

$$\mathcal{L} = C \prod_{l}^{11\ \text{enrichment}} \prod_{k}^{5\ \text{tagging}} \prod_{i}^{N_{kl}\ \text{events}} f_{kl}(x^{\rm eff}_{ik}, \mu_{ik}, t_i) \, , \tag{6}$$

where C is a constant independent of B oscillation frequencies and lifetimes, N_{kl} is the number of selected candidates from enrichment class l falling in tagging class k, and where

$$f_{kl}(x^{\rm eff},\mu,t) = \sum_{j}^{5\ \rm sources} Y_{jkl}(x^{\rm eff}) \left[\left(1 - X_{jk}(x^{\rm eff})\right) h_j(\mu,t) + X_{jk}(x^{\rm eff}) h_j(-\mu,t)\right] . \quad (7)$$

The event-by-event quantities $X_{jk}(x^{\rm eff})$ and $Y_{jkl}(x^{\rm eff})$ are computed from the distributions $G^c_{jk}(x^{\rm eff})$ and mistag probabilities η_{jk} introduced in Sect. 5,

$$X_{jk}(x^{\rm eff}) = \eta_{jk}\,\frac{G^-_{jk}(x^{\rm eff})}{G_{jk}(x^{\rm eff})}, \quad Y_{jkl}(x^{\rm eff}) = \alpha_{jkl}\,\frac{G_{jk}(x^{\rm eff})}{\sum_{j'} \alpha_{j'kl} G_{j'k}(x^{\rm eff})}, \quad (8)$$

where $G_{jk}(x^{\rm eff}) = (1-\eta_{jk})G^+_{jk}(x^{\rm eff}) + \eta_{jk}G^-_{jk}(x^{\rm eff})$ and where α_{jkl} are the source fractions, satisfying $\sum_{j=1}^{5 sources} \alpha_{jkl} = 1$. It is assumed that the probability density function $G_{jk}(x^{\rm eff})$ and the mistag η_{jk} are equal in all enrichment classes. It is also assumed that the resolution constants (S^α_ℓ and S^β_g) are the same for all classes.

7 Results

The negative log-likelihood is shown in Fig. 3 as a function of Δm_s for the physics parameters of Table 1. The global minimum is at 15.5 ps^{-1}, but is not significant enough to claim a signal. The likelihood remains constant beyond 20 ps^{-1}.

In order to calculate a limit and to facilitate combination with other analyses, the results are also presented in the form of an "amplitude plot" [15]. With this method the magnitude of B^0_s oscillations is measured at fixed values of the frequency Δm_s, using a modified likelihood function that depends on a new parameter, the oscillation amplitude $\mathcal{A}$. This is achieved by replacing the probability density function of the B^0_s and $\bar{B}^0_s$ sources given in Eq. (4) with

$$\frac{e^{-t_0/\tau_s}}{2\tau_s}\left[1 + \lambda\mathcal{A}\cos\left(\Delta m_s\, t_0\right)\right] . \quad (9)$$

For each value of Δm_s, the new negative log-likelihood is then minimised with respect to $\mathcal{A}$, leaving all other parameters (including Δm_s) fixed. The minimum is well behaved and very close to parabolic. At each value of Δm_s one can thus obtain a measurement of the amplitude with Gaussian error, $\mathcal{A} \pm \sigma^{stat}_{\mathcal{A}}$. If Δm_s is close to the true value, one expects $\mathcal{A} = 1$ within the total uncertainty; however, if Δm_s is far from its true value, a measurement consistent with $\mathcal{A} = 0$ is expected.

The amplitude fit results are displayed in Fig. 4 as a function of Δm_s. A peak in the amplitude can be been seen around 15.5 ps^{-1}, but it is in a region beyond the sensitivity and, as for the likelihood, not significant enough to claim a signal. Ignoring systematic uncertainties all values of Δm_s below 10.3 ps^{-1}are excluded at 95% CL. The sensitivity estimated from the data, taken as the value of Δm_s at which $1.645\sigma^{stat}_{\mathcal{A}} = 1$, is 11.0 ps^{-1}.

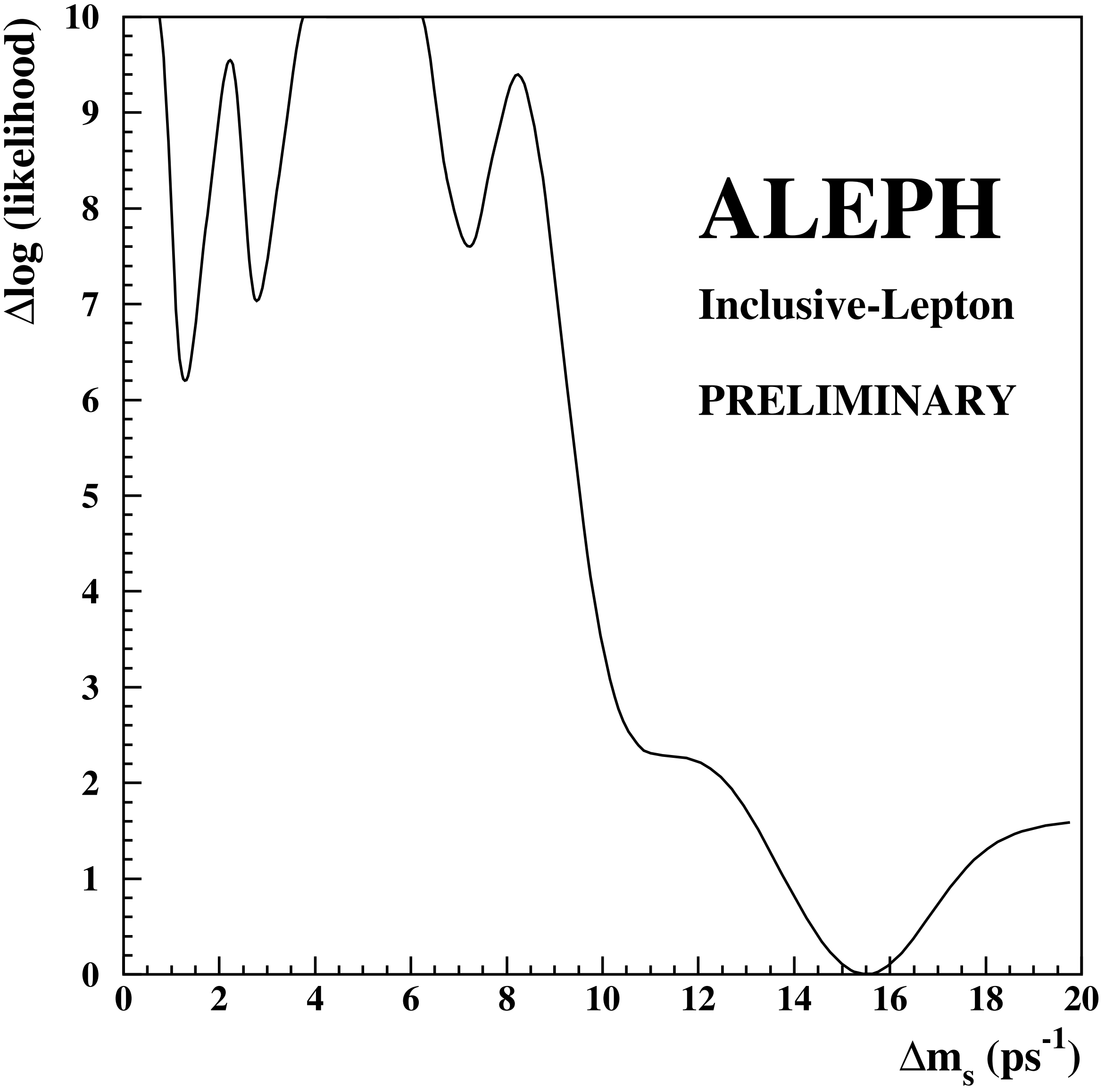

Figure 3: Negative log-likelihood difference with respect to the minimum as a function of Δm_s for this analysis.

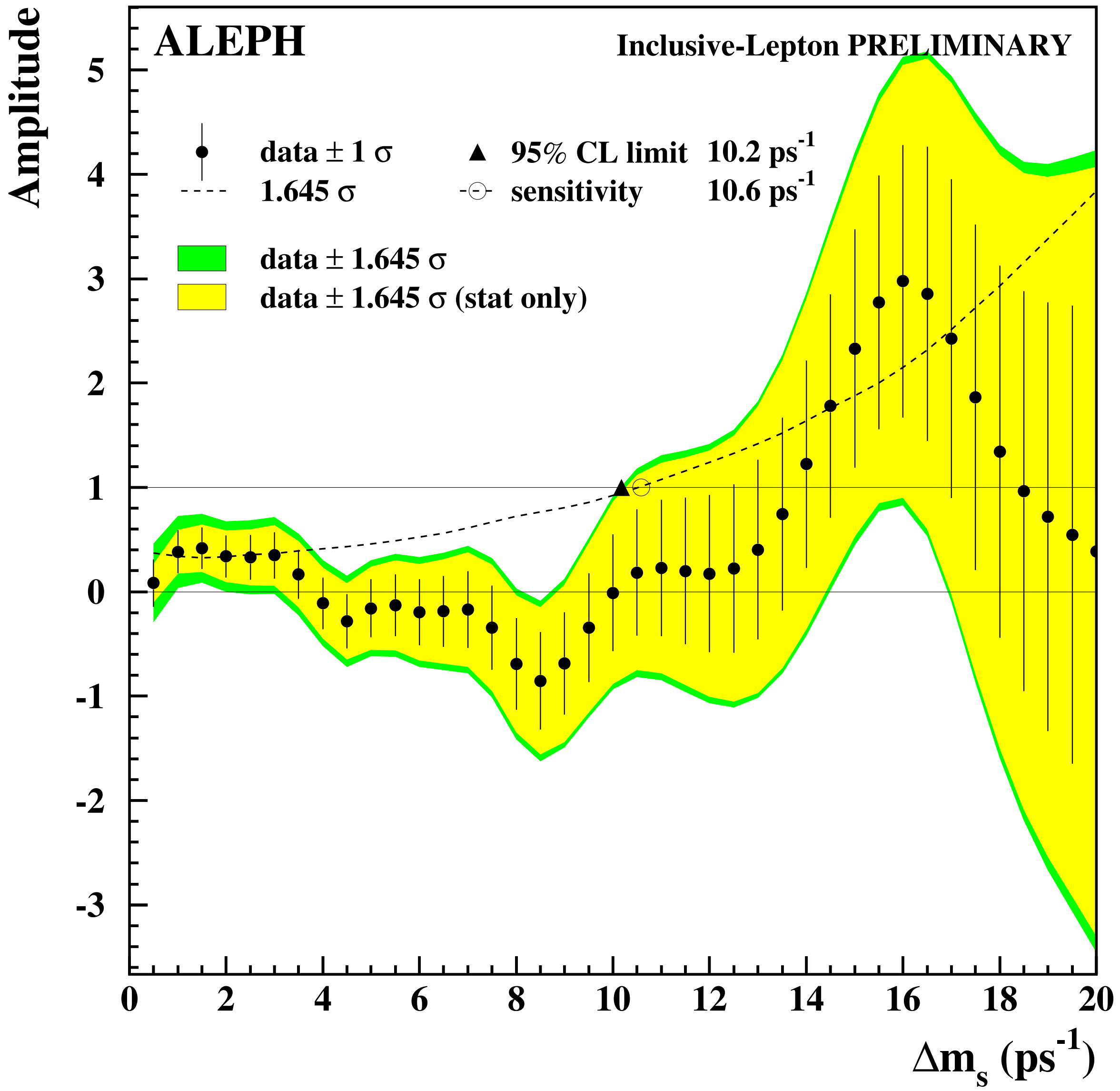

Figure 4: Measured amplitude as a function of Δm_s for this analysis. The error bars represent the 1σ total uncertainties, and the shaded bands show the one-sided 95% CL contour, with and without systematic effects included.

Table 5: Measurement of the B_s^0 oscillation amplitude $\mathcal{A}$ at $\Delta m_s = 9$ ps^{-1} together with the statistical uncertainty $\sigma_{\mathcal{A}}^{stat}$ and the total systematic uncertainty $\sigma_{\mathcal{A}}^{syst}$; a breakdown of $\sigma_{\mathcal{A}}^{syst}$ in several categories of systematics effect is also given.

Δm_s	9 ps^{-1}
$\mathcal{A}$	-0.685
$\sigma_{\mathcal{A}}^{stat}$	± 0.457
$\sigma_{\mathcal{A}}^{syst}$	$^{+0.181}_{-0.169}$
Systematics contributions :	
– $f_{B_s^0}$	$^{+0.111}_{-0.090}$
– $f_{b-baryon}$	$^{+0.030}_{-0.018}$
– $b \to \ell, b \to c \to \ell, b \to \bar{c} \to \ell, c \to \ell$	$^{+0.049}_{-0.010}$
– B_s^0 enrichment	$^{+0.057}_{-0.042}$
– efficiencies (MC stat.)	$^{+0.080}_{-0.051}$
– proper time resolution	$^{+0.087}_{-0.124}$
– tagging and discrimination	$^{+0.000}_{-0.015}$
– B-lifetimes and Δm_d	$^{+0.009}_{-0.016}$

8 Systematic errors and checks

The systematic uncertainties on the B_s^0 oscillation amplitude $\sigma_{\mathcal{A}}^{syst}$ are calculated, using the prescription in Ref. [15], as

$$\sigma_{\mathcal{A}}^{syst} = \mathcal{A}^{new} - \mathcal{A}^{nom} + (1 - \mathcal{A}^{nom})\frac{\sigma_{\mathcal{A}}^{new} - \sigma_{\mathcal{A}}^{nom}}{\mathcal{A}^{nom}}$$

where the superscript *nom* refers to the amplitude values and statistical uncertainties obtained using the nominal values for the various parameters and *new* refers to the new amplitude values obtained when a single parameter is changed. The total systematic uncertainty is the quadrature sum of the 1σ contributions of all the quantities considered in the systematic studies. The following systematic uncertainties are considered:

- **Sample composition:** The systematic uncertainty on the sample composition is obtained by varying the assumed values for the B hadron fractions $f_{B_s^0}$, $f_{b-baryon}$ and the various lepton sources ($b \to \ell$, $b \to c \to \ell$, etc ...) by the uncertainties quoted in Table 1.

  The systematic uncertainty due to the B_s^0 enrichment procedure is still preliminary. It is estimated by shifting the B_s^0 purity in each enrichment class in the direction of the average B_s^0 purity by $\pm 20\%$ of its difference with respect to the average.

  The statistical error on the efficiencies determined from the Monte Carlo are also propagated.

- **Proper time resolution:** For the systematic uncertainty on the proper time resolution the boost term resolution is given a relative variation of $\pm 10\%$ and the scale factor for the decay length resolution ($S_\ell^{dat} = 1.06 \pm 0.10$) is varied by its measured uncertainty.

- **Mistag:** The systematic uncertainties due to the mistag are also preliminary. A variation of three times the statistical uncertainity from the Monte Carlo is assumed. They corresponds to an absolute variation of 1.5% for tagging class 1 (opposite hemisphere charge), 3% for class 2 (fragmentation kaon), and 3.3% for class 3 (opposite lepton). These variations are similar to those used in the D_s^- based analyses. The changes in mistag arising as a consequence of varying the $b \to c \to \ell$ fraction are included as part of the sample composition systematic uncertainty.

- **Lifetimes and $\boldsymbol{\Delta m_d}$:** The various B lifetimes and the assumed value for Δm_d are varied within the uncertainties quoted in Table 1.

The relative importance of the various systematic uncertainties depends on Δm_s. Table 5 summarises the contributions for $\Delta m_s = 9$ ps^{-1}, a value close to the quoted limit. Except at small Δm_s the systematic uncertainties are generally small. The most important contributions are $f_{B_s^0}$ and the decay length resolution.

Including the systematic errors the limit and sensitivity obtained in the data are reduced to $\Delta m_s > 10.2$ ps^{-1} and 10.6 ps^{-1} respectively.

A straight line fit of the amplitude plot from the data is performed taking into account the statistical correlation between points. The average amplitude, in the range $0 \leq \Delta m_s \leq 10$ ps^{-1}, is found to be 0.085 ± 0.115, consistent with zero within the quoted uncertainty, as expected for no significant signal in this Δm_s range.

A likelihood fit on a $Z \to q\bar{q}$ Monte Carlo having the same statistics as the data and generated with a true value of Δm_s of 3.33 ps^{-1} yields $\Delta m_s = 3.32 \pm 0.11(\text{stat.})$ ps^{-1} in agreement with the input value. Performing an amplitude fit on the same Monte Carlo events yields the results shown in Fig. 5; as expected the amplitude is 1 at the the true value of Δm_s. The sensitivity estimated from this Monte Carlo (ignoring systematic uncertainties) is 11.6 ps^{-1} and is a little higher than that obtained in the data due to the slightly better decay length resolution in the Monte Carlo.

Using a fast Monte Carlo generator which takes into account all the details of the sample composition, the resolution functions, the mistag rates and the distributions of x^{eff}, the expectations $\mathcal{A} = 0$ and $\mathcal{A} = 1$ for the fitted amplitude have been checked. The average amplitude over many fast Monte Carlo experiments is indeed found to be consistent with unity for $\Delta m_s = \Delta m_s^{true}$ and with zero for any value of Δm_s if $\Delta m_s^{true} = \infty$.

As a further check of the assumed mistags and sample composition, exactly the same analysis is used to measure Δm_d in the data. Fixing Δm_s to 50 ps^{-1} and minimising the negative log-likelihood with respect to Δm_d gives $\Delta m_d = 0.477 \pm 0.025(\text{stat.})$ ps^{-1} consistent with the latest world average of 0.466 ± 0.019 ps^{-1} [11]. Figure 6 shows that the corresponding amplitude fit is consistent with that measured in the $Z \to q\bar{q}$ Monte Carlo and has the expected value of 1 at the minimum in the negative log-likelihood.

9 Combination with D_s^- analyses

As the statistical correlation between this analysis and the previous ALEPH dilepton analysis [3, 5] and lepton-kaon analysis [5] is expected to be large, these latter analyses

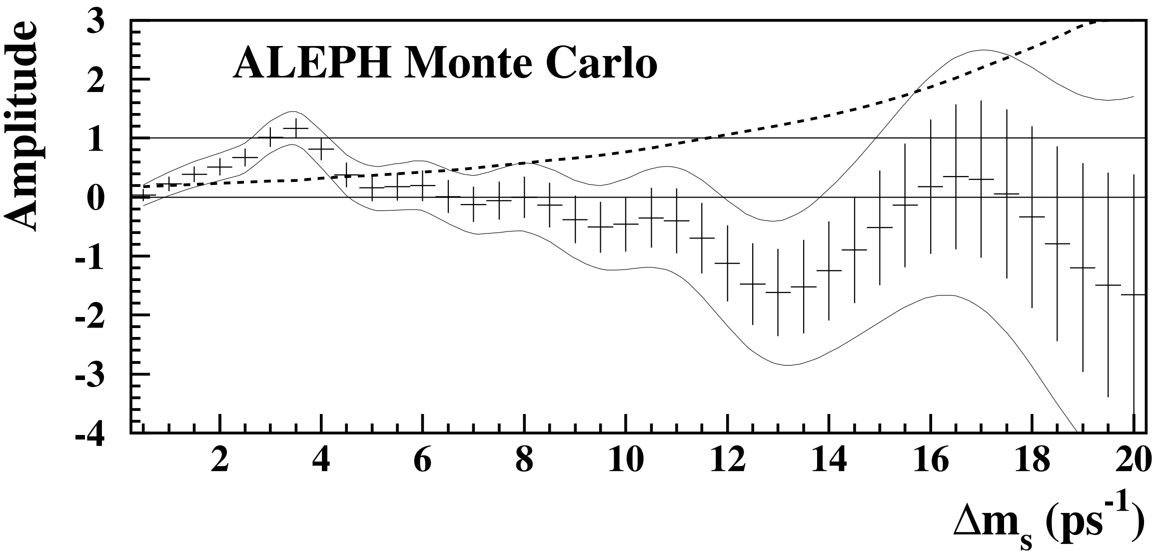

Figure 5: Measured amplitude as a function of Δm_s in the $Z \to q\bar{q}$ Monte Carlo. The error bars represent the 1σ statistical uncertainties, the full curve the one-sided 95% CL contour (systematic effects excluded). The dotted line is 1.645σ. The generated value of Δm_s was 3.33 ps^{-1}.

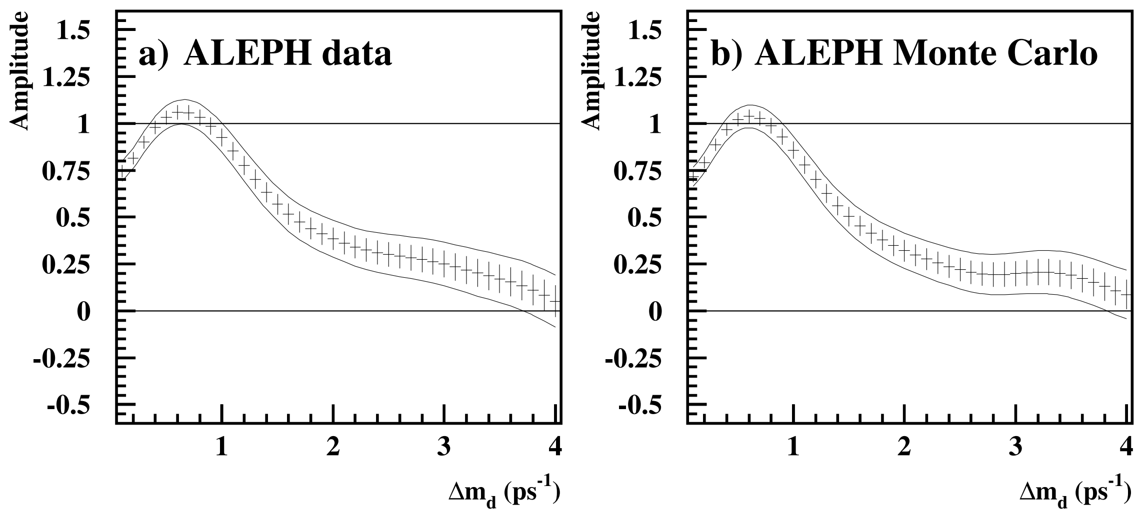

Figure 6: Measured amplitude as a function of Δm_d in (a) the data and (b) the $Z \to q\bar{q}$ Monte Carlo. The error bars represent the 1σ total uncertainties and the curves the one-sided 95% CL contour (systematic effects excluded).

are not included in this preliminary ALEPH combination.

Using a standard averaging procedure, the amplitudes measured in this analysis and in the two ALEPH D_s^- analyses are combined. The events common to both this analysis and the D_s-lepton analysis are removed from the inclusive lepton sample before combination. The following sources of systematic uncertainty are treated as fully correlated: the values assumed for $f_{B_s^0}$, $f_{B_d^0}$, Δm_d and the various B hadron lifetimes, the decay length resolution bias in the Monte Carlo simulation S_ℓ^{dat}, the mistag probabilities, and the use of the effective discriminating variable. Since the physics parameters assumed in the three analyses are slightly different, the D_s^- results are adjusted to the more recent set of physics parameters listed in Table 1 before averaging. The combined amplitude plot is displayed in Fig. 7. All values of Δm_s below 10.4 ps^{-1} are excluded at 95% CL. The combined sensitivity is estimated to be 11.7 ps^{-1}.

10 Conclusion

From a sample of 33000 inclusive lepton events, all values of Δm_s below 10.2 ps^{-1} are excluded at 95% CL using the amplitude method. This analysis supersedes the previous ALEPH inclusive lepton analysis [4]. When combined with the ALEPH D_s^- based analyses, the limit is $\Delta m_s > 10.4$ ps^{-1} at 95% CL.

References

[1] ALEPH Collaboration, Phys. Lett. B **377** (1996) 205.

[2] ALEPH Collaboration, "Study of B_s^0 oscillations using fully reconstructed D_s^- decays", Contribution PA95-611 to the 1997 EPS-HEP Conference, Jerusalem, Israel, 19-26 August 1997.

[3] ALEPH Collaboration, Phys. Lett. B **322** (1994) 441.

[4] ALEPH Collaboration, Phys. Lett. B **356** (1995) 409.

[5] ALEPH Collaboration, "Combined limit on the B_s^0 oscillation frequency", Contribution PA08-020 to the 28th International Conference on High Energy Physics, Warsaw, Poland, 25-31 July 1996.

[6] T. Sjöstrand and M. Bengtsson, Computer Phys. Commun. **43** (1987) 367.

[7] J. Körner and G. Schuler, Z. Phys. C **38** (1988) 511.

[8] ALEPH Collaboration, Z. Phys. C **53** (1992) 1.

[9] ALEPH Collaboration, Nucl. Instrum. Methods A **346** (1994) 461.

[10] J. Richman,"Progress in understanding heavy flavor decays" contribution to the 28th International Conference on High Energy Physics, Warsaw, Poland, July 1996.

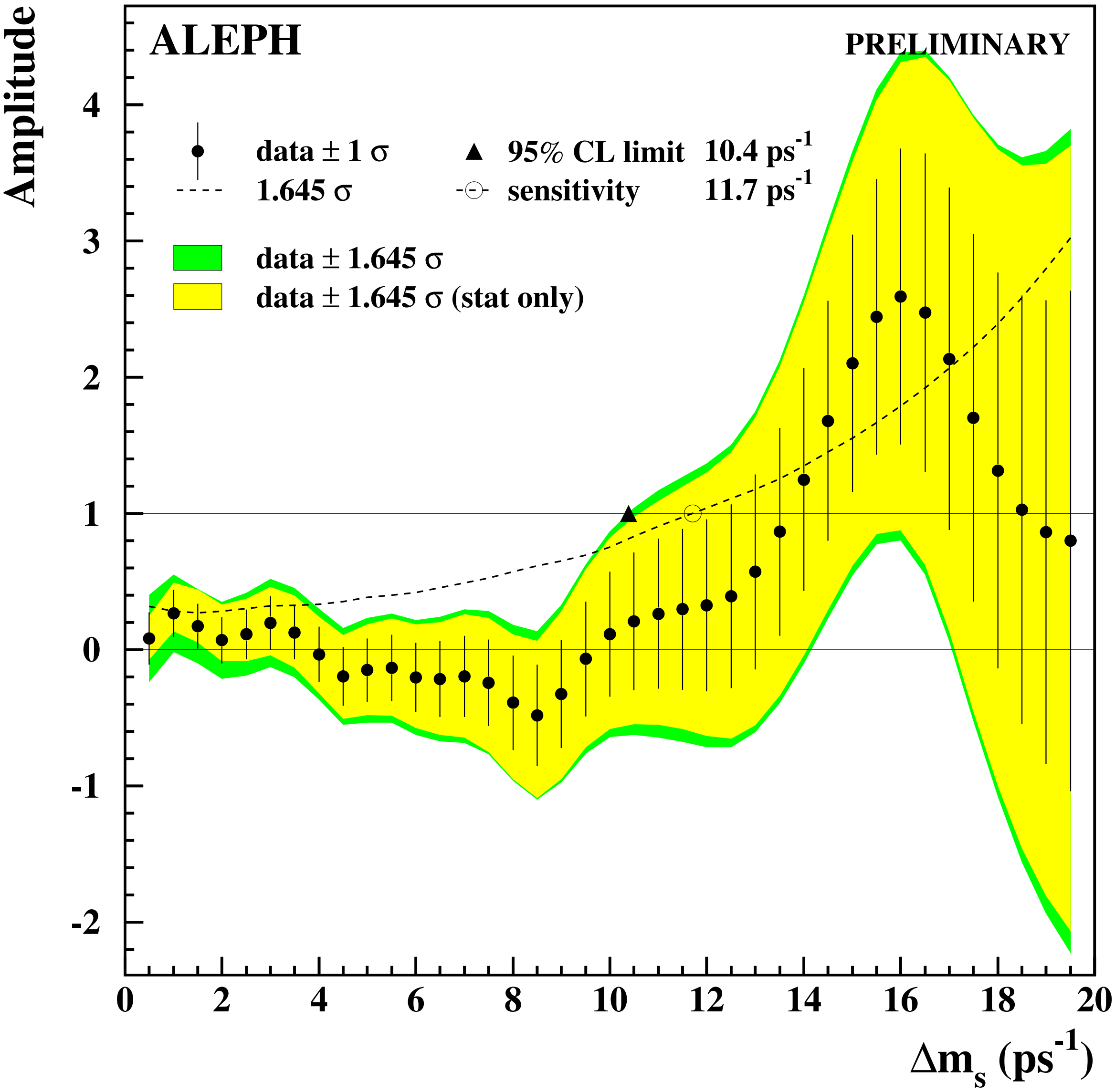

Figure 7: Measured amplitude as a function of Δm_s for the combination of this analysis with the ALEPH D_s^- based analyses.

[11] The LEP B Oscillations Working Group, "LEP Combined Results on B^0 Oscillations", LEPBOSC Note 97/1.

[12] ALEPH, DELPHI, L3, OPAL Collaborations and the SLD Heavy Flavour Group, "A combination of preliminary electroweak measurements and constraints on the Standard Model", LEPWWG/97-01.

[13] ALEPH, DELPHI, L3, OPAL Collaborations, Nucl. Instrum. Methods A **378** (1996) 101.

[14] ALEPH Collaboration, Phys. Lett. B **322** (1994) 275.

[15] H.-G. Moser and A. Roussarie, Nucl. Instrum. Methods A **384** (1997) 491.